Nov 24th, 12:00 AM

The Shear Flexibility of Corrugated Steel Sheeting

R. M. Lawson

J. Michael Davies

THE SHEAR FLEXIBILITY OF CORRUGATED STEEL SHEETING

by J M Davies BSc, PhD, MICE, MIStructE, CEng*

and R M Lawson BSc, ACGI**

1. Introduction

Corrugated steel sheeting possesses considerable strength and stiffness with respect to in-plane shear forces. This property has led to the increasing use of sheeting not merely as cladding but as an integral part of the structure. The simplest and possibly most important application is the use of an assembly of roof sheeting and its supporting members as a shear diaphragm as shown in Fig 1. The design of diaphragms for both flexibility and strength has been fully quantified analytically by Bryan[1] and refined by Davies[2] and it has been verified by extensive testing and comprehensive analysis that the flexibility 'c' of the complete assembly can be obtained as the sum of

$c_{1.1}$ = the flexibility due to distortion of the corrugation profile

$c_{1.2}$ = the flexibility due to shear strain in the sheeting

$c_{2.1}$ = the flexibility due to slip at the sheet/purlin fasteners

$c_{2.2}$ = the flexibility due to slip at the seam fasteners

$c_{2.3}$ = the flexibility due to movement in the connections to the rafters

c_{3} = the flexibility due to axial strain in the purlins

Each of these components of flexibility can be calculated from a simple expression. In particular, the expression for $c_{1.1}$ is:-

---

* Reader in Civil Engineering, University of Salford, Salford M5 4WT, England

** Research Student, University of Salford, Salford M5 4WT, England

$$c_{1.1} = \frac{0.144\, a\, d^4\, K}{E\, t^3\, b^3} \qquad \ldots\ (1)$$

where a and b are the overall dimensions of the diaphragm (Fig 1)

d = the pitch of the corrugations

E = Young's Modulus

t = the net thickness of the sheeting

K is a dimensionless constant which is a property of the cross-section of the sheeting and is independent of the length b of the diaphragm.

The value of K depends on the way the sheeting is fastened to the supporting structure. Values for all trapezoidal profiles in common use in Britain have been tabulated[1] for discrete fasteners in every, alternate and every third trough.

This paper is an attempt to assess the adequacy of equation 1 as a practical approach to diaphragm flexibility and, in particular, interest is concentrated on the tendency of K to vary with length b. In order to make this assessment it is necessary to consider how the true behaviour can be precisely defined. Three alternative approaches to the accurate determination of $c_{1.1}$ are discussed and typical results are compared. As a result of this comparison, the relative merits of these approaches are evaluated and an alternative expression for $c_{1.1}$ is suggested.

2. Approaches to the accurate determination of distortional flexibility

Distortional flexibility arises because the centre of shear resistance of the profile is eccentric to the plane of application of the applied shear force and the corrugation is twisted out of shape by its own shear flow. The individual plates, whilst moving laterally, also rotate and bend in plane thus giving rise to longitudinal warping with accompanying shear displacement of the sheeting.

This complex behaviour is greatly influenced by the arrangement of fasteners and other restraints at the ends of the corrugations. Attention here is concentrated on the typical case where the sheeting is fastened down to a supporting member by a discrete fastener in every trough. Similar arrangements, with fasteners in alternate or every third trough, give rise to much greater flexibilities and can be treated by extensions of the methods described here.

In the present state of the art, a precise and rigorous analysis cannot be made and there are three alternative approaches, each with its own particular advantages and disadvantages.

2.1 Energy methods of analysis

Energy methods of analysis are essentially approximate. Suitable displacement functions are assumed and the internal forces evaluated in terms of these displacements. The total potential energy of the system can then be evaluated and minimised with respect to each assumed displacement function, this yielding an assessment of the deformations of the system. Thus, in the particular case of interest, an estimate of the shear deformations in the sheeting can be found.

Evidently, energy methods depend for their accuracy on the validity of the assumed displacement functions and on any simplifying assumptions that are included in order to make the analysis tractable. Bryan's method[1] is essentially a very simple energy analysis in which only linear plate movements are considered as shown in plan in Fig 2. This is now known to be applicable only to relatively short lengths of sheeting. For longer lengths of sheeting, bending of the individual flat plates in their own plane leading to curvature of the fold lines renders Bryan's analysis invalid.

A much more comprehensive energy analysis by Libove[6] revealed the deficiencies of Bryan's approach and led to the present investigation. An alternative and equally comprehensive energy formulation is outlined in section 3 and forms the basis for the present study.

In many respects, energy methods offer the most satisfactory solution to the present problem but suffer from the disadvantage that unless an alternative precise method is available it is not clear what accuracy has been achieved and the relative merits of different approaches are difficult to assess.

2.2 Measurement of flexibility by testing

Clearly, the testing of actual panels of corrugated steel sheeting in shear presents an apparently attractive means of obtaining reliable data by which to judge the merits of the different analytical techniques. However, testing is not without its difficulties for the reasons which follow.

A fundamental difficulty in all of this work is the definition of the boundary conditions. If a single corrugation is considered it is clear that the longitudinal edge condition is different at the sides of the panel, where there is a tendency for the edge to be held straight by the framing members, to the condition internally, where there is a compatibility requirement with adjacent corrugations. Because of this situation, it is not possible to test a single corrugation. Instead a whole field of corrugations must be tested and it must be borne in mind that there will be corrugations at the edge of the field with non-typical boundary conditions.

Furthermore, experiments cannot be set up to measure $c_{1.1}$ in such a way that all of the other components of diaphragm flexibility ($c_{1.2}$ to c_3) are eliminated. Nevertheless,

testing provides a potentially reliable method of evaluating the distortional flexibility provided that the test set up is arranged in such a way that the other flexibility components are first minimised and then deducted analytically. It should be appreciated that the accuracy of this approach diminishes with increasing length as the magnitude of the distortional flexibility diminishes relative to the other components.

A suitable test apparatus is described in section 5 and some typical test results are presented in section 7.

2.3 Finite element methods

Provided that the correct boundary conditions are inserted, a finite element model provides the potentially most accurate method of evaluating the flexibility due to corrugation distortion. No overall assumptions are made regarding the pattern of displacements and provided that a sufficient number of elements are used the true behaviour can be examined under a range of external conditions.

A typical finite element model, in which a single corrugation is considered as a folded plate, is shown in Fig 3. It is evident that a considerable number of elements are necessary to model the long and narrow individual plates that make up the complete profile. As the simpler folded plate elements are only accurate at relatively low aspect ratios the size of the analysis becomes very large as the length of the corrugation increases.

For the finite element analysis described in section 6, the simplest suitable folded plate elements were used and a satisfactory arrangement of elements determined by a convergence study. It is considered that the results of this analysis provide a yardstick by which the accuracy of the other methods may be judged.

3. An Energy Method

The approach developed here is an extension of the method described by Horne and Raslan[4]. It has the advantage that the displacement functions are expressed as terms of a Fourier Series and the increase of accuracy may be examined as additional terms are included in the analysis.

It is assumed for the purpose of this study that a typical cross section of a corrugation can distort freely with the total displacement being expressed as individual plate displacements U_T, U_S and U_B as defined in Fig 4.

The individual plate displacements due to in-plane bending are expressed as a Fourier Series superimposed on the linear plate movements shown in Fig 2. Thus:-

$$\left.\begin{aligned} U_T &= a_1 y + a_2 \frac{b}{2\pi} \sin\frac{2\pi y}{b} + a_3 \frac{b}{4\pi} \sin\frac{4\pi y}{b} + a_4 \frac{b}{6\pi} \sin\frac{6\pi y}{b} \\ U_S &= a_5 y + a_6 \frac{b}{2\pi} \sin\frac{2\pi y}{b} + a_7 \frac{b}{4\pi} \sin\frac{4\pi y}{b} + a_8 \frac{b}{6\pi} \sin\frac{6\pi y}{b} \\ U_B &= a_9 \frac{b}{2\pi} \sin\frac{2\pi y}{b} + a_{10} \frac{b}{4\pi} \sin\frac{4\pi y}{b} + a_{11} \frac{b}{6\pi} \sin\frac{6\pi y}{b} \end{aligned}\right\} \quad \ldots\ (2)$$

where y is the distance along the corrugation measured from its centre line.

It may be noted at this stage that the influence of the supporting members resisting downward movement at the ends of the corrugations is considered in section 4 where an appropriate reduction factor is introduced.

In-plane shear strain γ in the plates is expressed by means of the relationships:

$$\gamma_T = \gamma_1 + \gamma_2 \cos \frac{2\pi y}{b}$$

$$\gamma_S = \gamma_3 + \gamma_4 \cos \frac{2\pi y}{b} \quad \ldots\ (3)$$

$$\gamma_B = \gamma_5 + \gamma_6 \cos \frac{2\pi y}{b}$$

The total deformation of the single corrugation is therefore expressed in terms of a set of functions with 17 variable coefficients which can be expressed in terms of a coefficient vector V where

$$V = a_1, a_2, \ldots\ a_{11}, \gamma_1, \gamma_2, \ldots\ \gamma_6 \quad \ldots\ (4)$$

It then follows from considerations of compatibility that the end shear displacement Δ, defined in Fig 2 is

$$\Delta = 2b_T (a_1 - a_2 + a_3 - a_4 + \gamma_1 - \gamma_2) + 4b_S (a_5 - a_6 + a_7 - a_8 + \gamma_3 - \gamma_4)$$
$$+ 2b_L (-a_9 + a_{10} - a_{11} + \gamma_5 - \gamma_6) \quad \ldots\ (5)$$

A necessary requirement for compatibility between adjacent corrugations is that the relative shear displacement between the two longitudinal edges should remain constant along the total length. This implies that equation (5) can be simplified thus:-

$$\Delta = 2b_T (a_1 + \gamma_1) + 4b_S (a_5 + \gamma_3) + 2b_L \gamma_5 \quad \ldots\ (6)$$

and that:

$$0 = 2b_T (a_2 + \gamma_2) + 4b_S (a_6 + \gamma_4) + 2b_L (a_9 + \gamma_6)$$

$$0 = 2b_T a_3 + 4b_S a_7 + 2b_L a_{10} \quad \ldots\ (7)$$

$$0 = 2b_T a_4 + 4b_S a_8 + 2b_L a_{11}$$

The total strain energy of the deformed corrugation may be expressed as the sum of the energies due to:-

(a) bending of the cross-section

(b) longitudinal bending of the plate elements

(c) longitudinal axial strains in the plate elements

(d) shear strain in the plate elements

3.1 Bending of the Cross Section

The bending or distortional energy at any cross-section arises as a result of the portal frame-like movements associated with U_T, U_S and U_B. It follows that the bending moment at any point can be expressed in terms of these three parameters and the total strain energy of bending obtained by integrating around the section and along the length. Thus the distortional strain energy E_D may be expressed as

$$E_D = \int_0^b \Big[C(1,1)\, U_T^2 + C(1,2)\, U_S U_T + C(1,3)\, U_T U_B + C(2,2)\, U_S^2 + C(2,3)\, U_S U_B + C(3,3)\, U_B^2 \Big] dy \quad \ldots\ (8)$$

where $C(1,1)\ldots$ etc are readily derived[4] functions of the cross-sectional dimensions b_T, b_S, b_L etc and the plate bending stiffness $Et^3/12$.

A typical integration within equation 8 takes the form

$$\int_0^b C(1,2)\, U_S U_T\, dy = C(1,2) \Big[\frac{b^3}{(2\pi)^2} (a_1 a_6 + a_2 a_5) + \frac{b^3}{2(2\pi)^2} a_2 a_6 - \frac{b^3}{(4\pi)^2} (a_1 a_7 + a_3 a_5) + \frac{b^3}{2(4\pi)^2} a_3 a_7 + \frac{b^3}{(6\pi)^2} (a_4 a_5 + a_1 a_8) + \frac{b^3}{2(6\pi)^2} a_4 a_8 \Big] \quad \ldots\ (9)$$

3.2 Longitudinal bending of the plate elements

The longitudinal bending strain energy is given by

$$E_B = \sum_i \frac{E I_i}{2} \int_0^b \left(\frac{d^2 U_i}{dy^2} \right) dy \qquad \ldots\ (10)$$

where i refers to the top, side and bottom plates respectively.

$$\therefore\ E_B = \frac{2\pi^2 Et}{3b} \left[b_T^3 (a_2^2 + 4a_3^2 + 9a_4^2) + 2b_S^3 (a_6^2 + 4a_7^2 + 9a_8^2) + b_L^3 (a_9^2 + 4a_{10}^2 + 9a_{11}^2) \right] \qquad \ldots\ (11)$$

3.3 Longitudinal axial strains in the plate elements

The bending displacements giving rise to the above expression for E_B imply a potential incompatibility of longitudinal strain at the plate joints. It is therefore necessary to include an additional energy term corresponding to the appropriate membrane extension of the side plate which takes the form

$$E_L = \frac{\pi^2 b_S Et}{b} \left[(a_2 b_T - a_9 b_T + b_T \gamma_2 - b_L \gamma_6)^2 + 4(a_3 b_T - a_{10} b_L)^2 + 9(a_4 b_T - a_{10} b_L) \right] \qquad \ldots\ (12)$$

3.4 Shear strain in the plate elements

Here, the total strain energy is

$$E_S = \frac{G}{2} \int_0^S \int_0^b \gamma^2 ds\, dy$$

$$= Gtb \left[b_T \gamma_1^2 + \frac{b_T}{2} \gamma_2^2 + 2b_S \gamma_3^2 + \frac{b_S}{2} \gamma_4^2 + b_L \gamma_5^2 + \frac{b_L}{2} \gamma_6^2 \right] \qquad \ldots\ (13)$$

3.5 Summation of the energy expressions and solution for $c_{1.1}$

An examination of equations (8), (9), (11), (12) and (13) reveals that the total energy E may be expressed as follows

$$E_{Tot} = E_D + E_B + E_L + E_S$$
$$= V \left[D \right] V^T \quad \ldots\ (14)$$

where V is the vector of coefficients in the displacement functions (equation (4)) and $\left[D \right]$ is a square symmetric matrix of coefficients dependent only on the dimensions of the corrugation.

The minimum potential energy condition is obtained by minimising the energy with respect to variations of each of the displacement coefficients.

Thus,

$$dE = 2da_i \quad D_i \quad V^T = 0 \quad \ldots\ (15)$$

where da_i are small variations in each of the displaccment coefficients a_1, a_2, ... γ_6 in turn and D_i is a vector of the terms in row i of $\left[D \right]$.

It may be noted that the compatibility conditions (implied in equation (6) and given in equations (7) demand that 4 of the coefficients are not independent and the 17 equations (15) may be reduced by 4 using equations (6) and (7) and their differentiated form shown below.

$$
\left.
\begin{aligned}
da_5 &= -\frac{b_T}{2b_S}\, da_1 - \frac{b_T}{2b_S}\, d\gamma_1 - d\gamma_3 - \frac{b_L}{2b_S}\, d\gamma_5 \\
da_9 &= -\frac{b_T}{b_L}\, da_2 - \frac{b_T}{b_L}\, d\gamma_2 - \frac{2b_S}{b_L}\, da_6 - \frac{2b_S}{b_L}\, d\gamma_4 - d\gamma_6 \\
da_{10} &= -\frac{b_T}{b_L}\, da_3 - \frac{2b_S}{b_L}\, da_7 \\
da_{11} &= -\frac{b_T}{b_L}\, da_4 - \frac{2b_S}{b_L}\, da_8
\end{aligned}
\right\} \quad \ldots\ (16)
$$

This gives a set of 13 simultaneous equations in the 13 independent coefficients. These may be expressed in matrix form as

$$\left[H\right]\ \bar{a} = B \qquad \ldots\ (17)$$

where $\left[H\right]$ is a square symmetric matrix and B a column vector both involving only the dimensions of the corrugation and where

$$\bar{a} = \begin{bmatrix} a_1/\Delta \\ a_2/\Delta \\ a_3/\Delta \\ a_4/\Delta \\ a_6/\Delta \\ a_7/\Delta \\ a_8/\Delta \\ \gamma_1/\Delta \\ \vdots \\ \gamma_6/\Delta \end{bmatrix} \qquad \ldots\ (18)$$

These equations can be solved for the coefficients a_1/Δ .... etc. When the values obtained are substituted back into the expression for the total energy E, the shear flexibility c is obtained as

$$c = \frac{\Delta^2}{2E_{Tot}} \quad \ldots\ (19)$$

To extract the distortional shear flexibility $c_{1.1}$ from c, the pure shear flexibility $c_{1.2}$ must be subtracted where

$$c_{1.2} = \frac{2\ (b_L + 2b_S + b_T)}{t\ b\ G} \quad \ldots\ (20)$$

3.6 Influence of the number of Fourier terms

If, in the analysis described above, only a_1 and a_5 are retained and the remaining variable coefficients a_2, a_3 .... etc removed from the analysis, Bryan's analysis[1] leading to equation (1) is obtained. Fig 5 shows how, in a typical analysis, an increase in the number of Fourier terms results in an increase in the distortional flexibility and hence in the apparent value of the sheeting constant K. It is very clear that as the length of the corrugation increases more terms are required to accurately reproduce the displacement pattern. Physically, as the length increases, the non-linear part of the total distortion becomes more concentrated near the ends of the corrugation and more terms are required to reproduce this behaviour.

The most important single factor in the increase of K with length appears to be the horizontal displacement U_B of the bottom plate. If a_9, a_{10}, a_{11} are removed from the analysis a large reduction in K is obtained, in many cases reducing K almost to its base value (Bryan's theory). It is apparent that in a real situation, where the sheeting may be fastened to intermediate purlins as well as at its ends,

horizontal movement of the bottom plate will be restrained and a reduction of K may be expected. Initial investigations suggest that at least two intermediate purlins are required before this reduction becomes significant and pending further study, it is suggested that the effect be ignored.

4. The effect of supporting members at the corrugation ends

Corrugation distortion reaches a maximum at the ends of the corrugations and any factors that influence the patterns of displacement in these critical areas may have a significant influence on the shear flexibility. In section 3 it was assumed that complete freedom of vertical movement existed at the bottom of the side plates over the whole length of the corrugation whereas Fig 6 shows that, at the ends of the corrugations, vertical downward movement is prevented by the presence of the supporting members.

This leads to a reduction of shear flexibility which may be accounted for by multiplying the value obtained according to section 3 by a factor (1 - r) where r is a reduction factor that has been found to be very nearly constant with length. Edge beam reduction factors can thus be readily calculated on the basis of linear plate displacements and values calculated on this basis[5] will be utilised to modify the predictions of section 3 in the subsequent discussion.

Naturally, finite element methods can take account of this effect and this allows the accuracy of the reduction factor approach to be evaluated more precisely in section 7.

5. Experimental determination of flexibility

Some of the difficulties inherrent in the determination of $c_{1.1}$ by testing have been

outlined in section 2.2, and means of overcoming them suggested. A suitable arrangement for a test programme is shown, without any sheeting in place in Fig 7. The left hand longitudinal member and the jacking point were bolted down to the strong floor of the Structures Laboratory at the University of Salford. The right hand longitudinal member was free to move over needle bearings on the supports. The following points may be noted:-

(a) The framing members were of substantial proportions in order to minimise flexibility due to axial strain.

(b) The joints between framing members were pinned so that the unclad rig had negligible stiffness.

(c) Provision was made to measure any rigid body rotation of the rig as a whole.

(d) Provision was made to vary the width of the rig so that widths from 150mm (single corrugation) to 1250mm (7 or 8 corrugations according to pitch) could be tested.

(e) Provision was made to vary the length of the rig from 1 to 6 metres in steps of 1 metre. In Fig 7, intermediate purlins are shown in all possible positions. In any test only purlins at the ends of the sheet would be in place together with a single purlin at midspan to prevent excessive sagging.

(f) The tops of the purlins were set at the same level as the tops of the rafters in order to minimise any eccentricities of loading.

(g) Where seams between adjacent sheet widths were necessary, a large number of seam fasteners were used in order to minimise the influence of slip in these fasteners.

Three separate sheet profiles, each of 35mm depth, were used in the test series described in this paper. In Fig 8 the entire rig is shown clad with British Steel Corporation Longrib 700 decking. Tests were also carried out with this same profile inverted to form a sheeting and with an intermediate profile (Briggs Amasco profile ST 35) as shown in Fig 9. Details of these profiles are shown on Figs 10 to 13.

Each profile was tested in order to establish the flexibility over the whole range from one to six metres. In general the full width of the rig was used but in the case of the Briggs Amasco sheeting, widths of one corrugation and four corrugations were tested as well as the full width of eight corrugations. For each test the load was increased in increments and then unloaded several times until a steady linear response was obtained so that the bedded-in value of fastener flexibility could be confidently used in subsequent analysis[3].

For each test the components of shear deflection other than that due to corrugation distortion were calculated according to current theory[2] and deducted from the measured deflection. The results of these tests are presented, together with appropriate theoretical comparisons, in Figs 11, 12 and 13. In each case the results are presented as effective values of the sheeting constant K assuming equation (1) to hold good.

6. Finite Element Analysis

For the analyses described in this paper, simple rectangular elements were used as shown in Fig 3, each element having five degrees of freedom per node[7]. The finite element mesh was generated by a specially written data generator which avoided tedious checking and eliminated the possibility of data errors. Each

complete corrugation required only four data cards to describe its boundary conditions, length and cross-sectional geometry, material properties and the way it was divided up into elements.

Of particular note in Fig 3 is the provision of edge members having high axial stiffness and zero bending stiffness in order to ensure compatibility of edge strain with adjacent corrugations. These correspond to the assumption of constant relative shear displacement between the two edges of the corrugation that was made in section 3 leading to equations (6) and (7) and represent the only method discovered to date of obtaining the necessary compatibility with adjacent corrugations.

The provision of the roller supports R shown in Fig 3 is optional in the data generator which can also deal with the case of the edges held straight. Thus all the cases necessary for a useful comparison with experiment and energy methods are available using finite elements though at a substantial cost in computing time as the number of degrees of freedom can quickly run to several thousand.

6.1 Convergence tests

In order to establish a suitable arrangement of elements, convergence tests were carried out for the two sheeting profiles used in the test series described in section 5. A length of 4 metres was chosen as being reasonably representative of the range of interest and an analysis carried out with 1, 2, 3 and 4 elements per face around the perimeter of the profiles and 60 elements in the length. As can be seen in table 1, the flexibility, expressed in terms of the apparent value of the sheeting constant K, is remarkably insensitive to the number of elements per face. Because any increase in the number of elements per face itself causes a dramatic rise in computing costs

as well as necessitating an increase in the number of elements in the length in order to preserve a satisfactory aspect ratio, it is advantageous to keep the number of elements per face to a minimum. On the basis of this convergence study, there appeared to be no advantage gained by having more than one element per face but this seemed a little unrealistic bearing in mind the simple elements used. It was accordingly decided to standardise on two elements per face for the remainder of the work.

Number of elements per face	Apparent value of K	
	Longrib 700 sheeting	Briggs Amasco ST35
1	.903	1.797
2	.898	1.791
3	.900	1.787
4	.899	1.782

Table 1 Convergence Tests - Varying number of elements per face

Further convergence tests were then carried out varying the number of elements along the length from 30 to 120 in steps of 30. The results of this investigation are plotted in Fig 10. It was clear that 90 to 120 elements were necessary for full convergence but that results sufficiently accurate for practical purposes could be obtained with 60 elements in the length. It was therefore decided to adopt 60 elements in the length (i.e. 600 elements in total) for a length of 4 metres and to maintain this element size for the other analyses (e.g. 30 elements x 2 per face = 300 for a length of 2 metres and 90 elements x 2 per face = 900 for a length of 6 metres).

The results of the finitc element analyses described are incorporated with the test results and the energy method analyses in Figs 11, 12 and 13.

7. Comparison of experimental and theoretical results

A full comparison of experimental and theoretical results for the three profiles is given in Figs 11, 12 and 13. In the case of the Briggs Amasco sheet, Fig 13, comparisons with the work of Libove[6] are also included.

From these graphs it can be concluded that:-

(a) In the absence of the supporting member effect, agreement between energy methods and finite element methods is good and the refinement of finite element methods is unnecessary for practical purposes.

(b) The reduction factor (section 4) gives an adequate account of the influence of the supporting members over the range of lengths considered.

(c) In the comparisons made to date, the energy method outlined in this paper has given similar results to Libove's somewhat different method[6] and the two must be considered equivalent.

(d) With the full width of the test rig, the experimental flexibilities lie remarkably close to the theoretical values with edge member effect included. This is considered to add further weight to the evidence that proves the adequacy of the energy approach described in this paper.

(e) As the number of corrugations considered reduces, the experimental flexibilities also reduce becoming very close to the edges held straight condition for a single corrugation.

(f) Over the practical range of lengths (length greater than 1.5 metres) the

variation of the sheeting constant K with length is almost exactly a straight line through the origin whether or not the influence of the supporting member is considered. This suggests that equation (1) may be profitably modified and such a modification is considered in section 8.

8. Suggested improvements to the expression for $c_{1.1}$

In section 7, it was shown that for all practical purposes, K is proportional to length and this suggests that equation (1) requires modification so that b^2 rather than b^3 should appear in the denominator. As this consideration arose out of a study of the variation of K with length it was decided to continue the parametric study and to consider the variation of K with thickness, other quantities being held constant. The energy method was used for this study and typical results are shown in Fig 14 for the range of interest ($0.5\text{mm} \leq t \leq 1.25\text{mm}$).

It was found that K was not constant with thickness t as implied in equation (1) but tended to vary with $\sqrt{t}$. As the d^4 term in equation (1) is in fact a cross-sectional dimension that exists to preserve the dimensional integrity of the equation, it follows that a better equation for the distortional flexibility may well be:-

$$c_{1.1} = \frac{a\, d^{2.5}\, \bar{K}}{E\, t^{2.5}\, b^2} \qquad \ldots\ (21)$$

In the above equation, $\bar{K}$ is alternative dimensionless sheeting constant which reflects the longitudinal bending properties of the profile as well as the cross-sectional bending properties.

Further investigation of equation (21) confirms its suitability for dealing with the variation of flexibility with length over a range of situations and it is now suggested that it should replace equation (1) for the case of sheeting fastened in every corrugation.

In order to facilitate the practical use of equation (21), Table 2 has been prepared from which the constant K may be extracted with adequate accuracy for most commercially available profiles. In table 2, the reduction factor r for the effect of the supporting member is also incorporated.

For the other important cases of sheeting fastened with a discrete fastener in alternate and every third corrugation it appears that the divergence with equation (1) is not so marked and that, pending the completion of the study of this case, the existing theory may be used.

Conclusions

The distortional shear flexibility of corrugated steel sheeting has been examined in detail using each of the analytical and experimental techniques currently available. It is concluded that a comprehensive energy analysis with a suitable reduction factor to allow for the supporting members at the ends of the corrugations provides a more than adequate prediction of the required flexibility and leads to a much improved expression for general use which accurately reflects the influence of panel length. Tables have been prepared which permit this improved expression to find immediate practical implementation.

Acknowledgement

Materials for the test programme described in this paper were provided by CONSTRADO as part of their continuing support for research into aspects of "stressed skin" and "frameless" construction using corrugated steel sheeting. This research is continuing at the University of Salford.

Summary

Distortional shear flexibility is an important part of the total flexibility of diaphragms fabricated using corrugated steel sheeting. A number of analytical techniques for determining this flexibility are available though their relative merits are not clear. In this paper, a further energy method of analysis is described and its accuracy justified by comparison with experiment and finite element analysis. The results included provide a yardstick by which other methods may be judged and a limited number of such comparisons are made.

As a result of this work, a simple expression for shear flexibility is developed and tables provided so that it can find immediate application in practical situations.

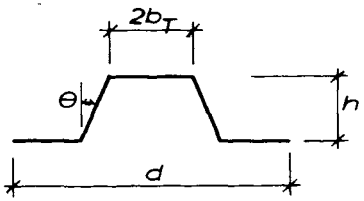

$$c_{1.1} = \frac{a\,d^{2.5}\,\bar{K}}{E\,t^{2.5}\,b^{2}}$$

h/d \ 2bI/d	0.1	0.2	0.3	0.4	0.5	0.6	0.7	0.8	0.9
0.1	.014	.033	.047	.053	.051	.048	.066	.075	.100
0.2	.047	.111	.158	.179	.178	.180	.227	.273	.374
0.3	.097	.222	.318	.364	.360	.369	.436	.570	.815
0.4	.172	.371	.523	.599	.597	.613	.754	.973	1.65
0.5	.244	.564	.862	.896	.878	.908	1.10	1.49	2.20

$\theta = 0°$

h/d \ 2bI/d	0.1	0.2	0.3	0.4	0.5	0.6	0.7	0.8	0.9
0.1	.017	.035	.046	.048	.043	.051	.059	.070	.109
0.2	.071	.121	.150	.153	.142	.166	.198	.247	
0.3	.162	.249	.288	.282	.261	.325	.383	.521	
0.4	.259	.408	.448	.438	.396	.505	.595		
0.5	.449	.593	.669	.541	.540	.699	.841		

$\theta = 15°$

h/d \ 2bI/d	0.1	0.2	0.3	0.4	0.5	0.6	0.7	0.8
0.1	.022	.036	.044	.042	.035	.045	.052	.076
0.2	.090	.121	.129	.119	.097	.132	.164	
0.3	.190	.224	.204	.188	.190	.205		
0.4	.323	.294	.225	.203	.184			
0.5	.357	.293	.189	.133				

$\theta = 30°$

h/d \ 2bI/d	0.1	0.2	0.3	0.4	0.5	0.6	0.7
0.1	.026	.037	.039	.033	.033	.037	.057
0.2	.100	.098	.089	.066	.065		
0.3	.134	.107	.049				
0.4	.065						

$\theta = 45°$

Table 2 Values of $\bar{K}$ including reduction factor for effect of supporting member

References

1. E R Bryan — "The stressed skin design of steel buildings" Crosby Lockwood Staples. London (1972).

2. J M Davies — "The design of shear diaphragms of corrugated steel sheeting" University of Salford Report Ref. No 74/50 (Sept 1974).

3. J M Davies and F Thompson — "Light gauge steel folded plate construction" Proc. 3rd Speciality Conf. on Cold Formed Steel Structs. Rolla Missouri (Nov 1975).

4. M R Horne and R A S Raslan — "An energy solution to the shear deformation of corrugated plates" Publications Int. Assn. of Bridge and Structural Engineers (31-I/1971).

5. R M Lawson — "Some practical design factors for the shear flexibility of corrugated sheeting" University of Salford Report Ref No 74/51 (Sept 1974).

6. C Libove and M J Hussain — "Stress and stiffness data for discretely attached corrugated shear webs with trapezoidal corrugations" Syracuse University. Report No MAE 5170-T3 (Dec 1974).

7. K C Rockey and H R Evans — "A finite element solution for folded plate structures" Int. Conf. on Space Structs. University of Surrey (1966)

Symbols

a = width of shear panel measured across the corrugations (mm)

$\bar{a}$ = vector of coefficients in the displacement functions

$a_1, a_2 \ldots$ = coefficients in the displacement functions

b = length of shear panel measured along the corrugations (mm)

b_L, b_S, b_T = cross-sectional dimensions defined in Fig 4

B = column vector of coefficients in the dimensions

c = flexibility of shear panel (mm/kN)

$c_{1.1}, c_{1.2} \ldots$ = components of shear flexibility

$C(1,1)$, $C(1,2)$ .... = terms involving cross-sectional dimensions only

d = pitch of corrugations (mm)

D = matrix of coefficients in the energy analysis

E = Young's modulus (kN/mm^2)

E_D, E_B .... = components of total strain energy

G = shear modulus

H = matrix of coefficients in the energy analysis

I = second moment of area

K, $\bar{K}$ = non-dimensional sheeting constants

r = reduction factor to allow for the influence of supporting members

t = net sheeting thickness (mm)

U_B, U_S, U_T = components of displacement defined in Fig 4

V = vector of coefficients in the displacement functions

y = distance along corrugation measured from centre line

γ = shear strain

$\gamma_1, \gamma_2, \ldots$ = coefficients in the assumed strain functions

Δ = shear displacement of corrugation

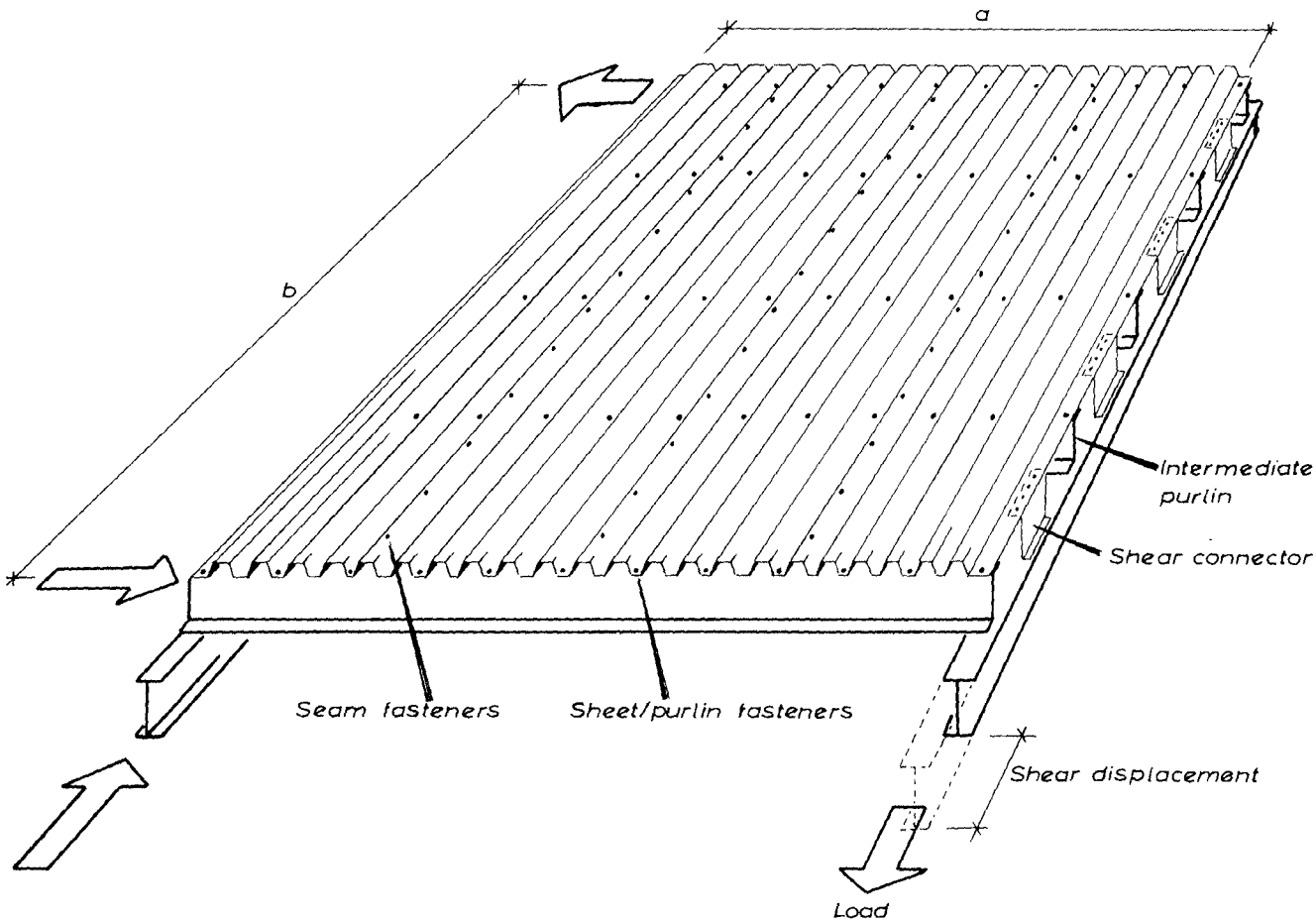

Fig 1 TYPICAL SHEAR DIAPHRAGM

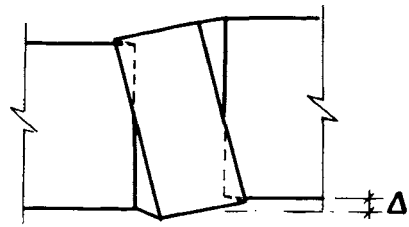

Fig 2 Distortion of corrugation in plan.
(with fold lines remaining straight)

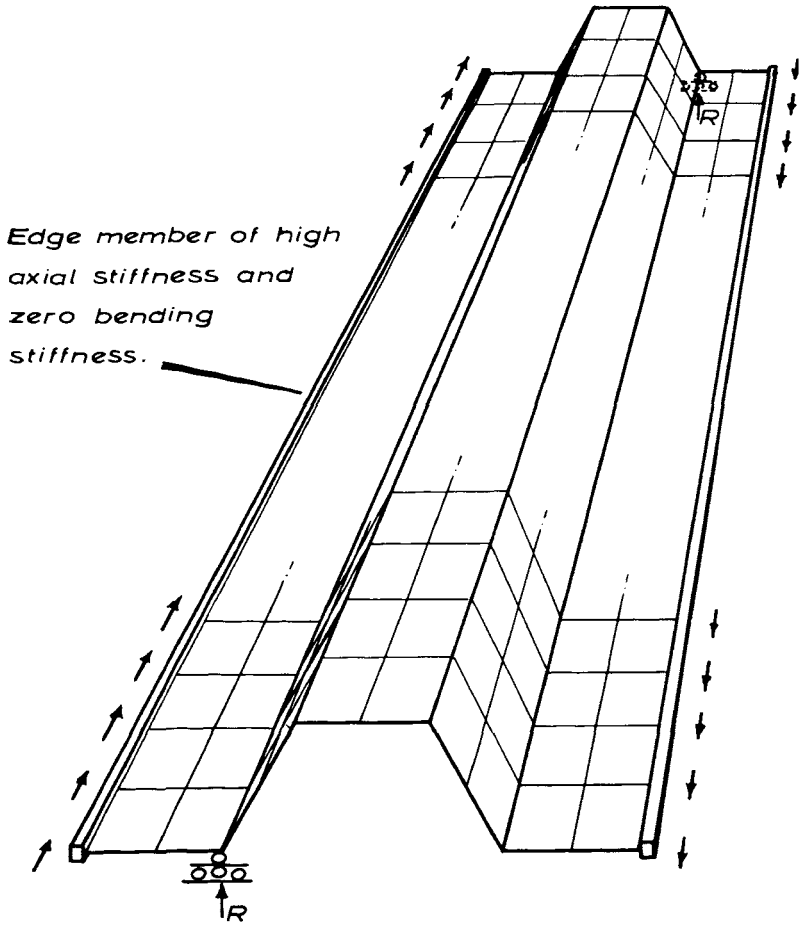

Fig 3 Finite element model of a single corrugation

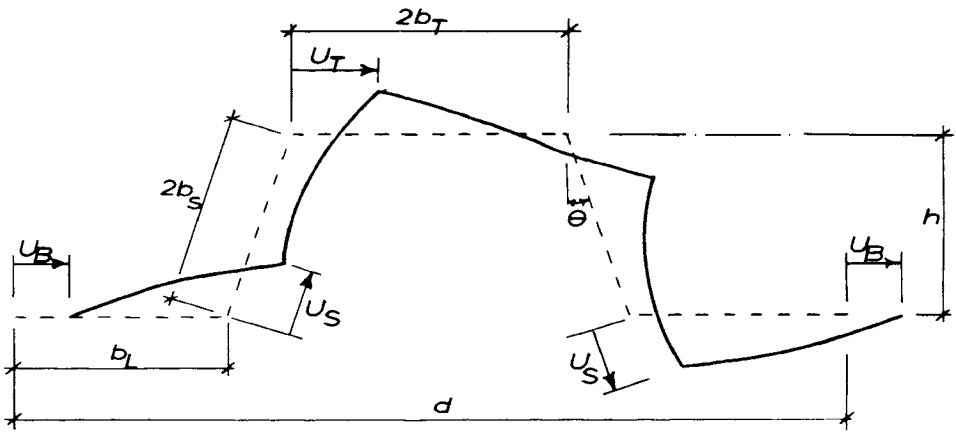

Fig 4 Profile dimensions and displacements.

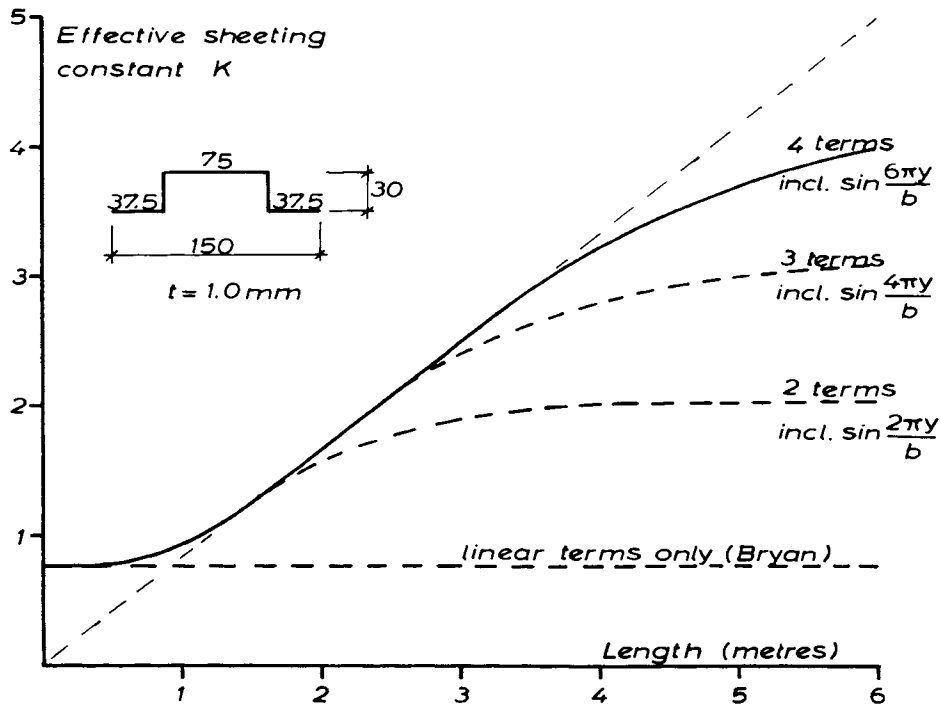

Fig 5 Illustrating the effect of increasing the number of Fourier terms in the plate displacement functions

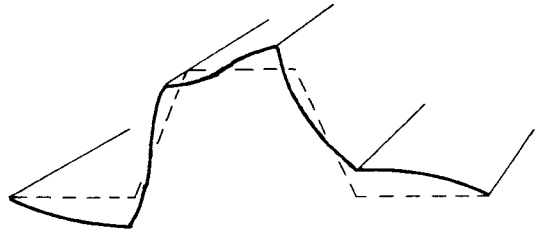

(a) Deformations assumed in energy analysis.

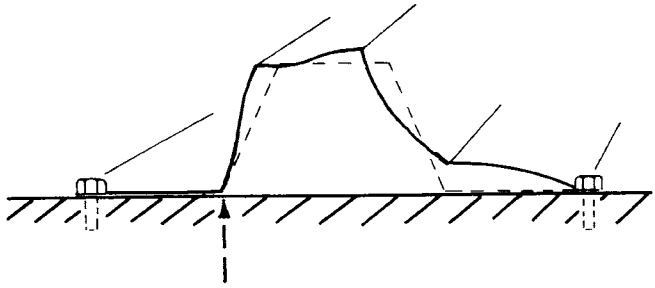

(b) Real situation - deformation restrained by supporting member.

Fig 6 Deformations at the end of a corrugation

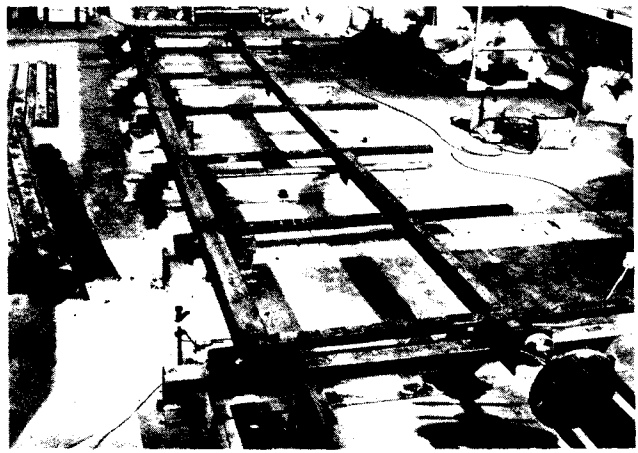

Fig 7 Test rig unclad

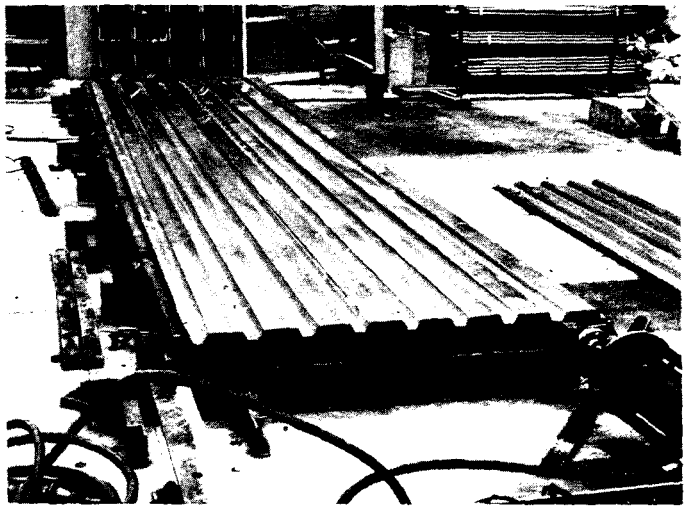

Fig 8 Test rig clad with BSC Longrib 700 decking

Fig 9 Test rig clad with Briggs Amasco profile ST 35

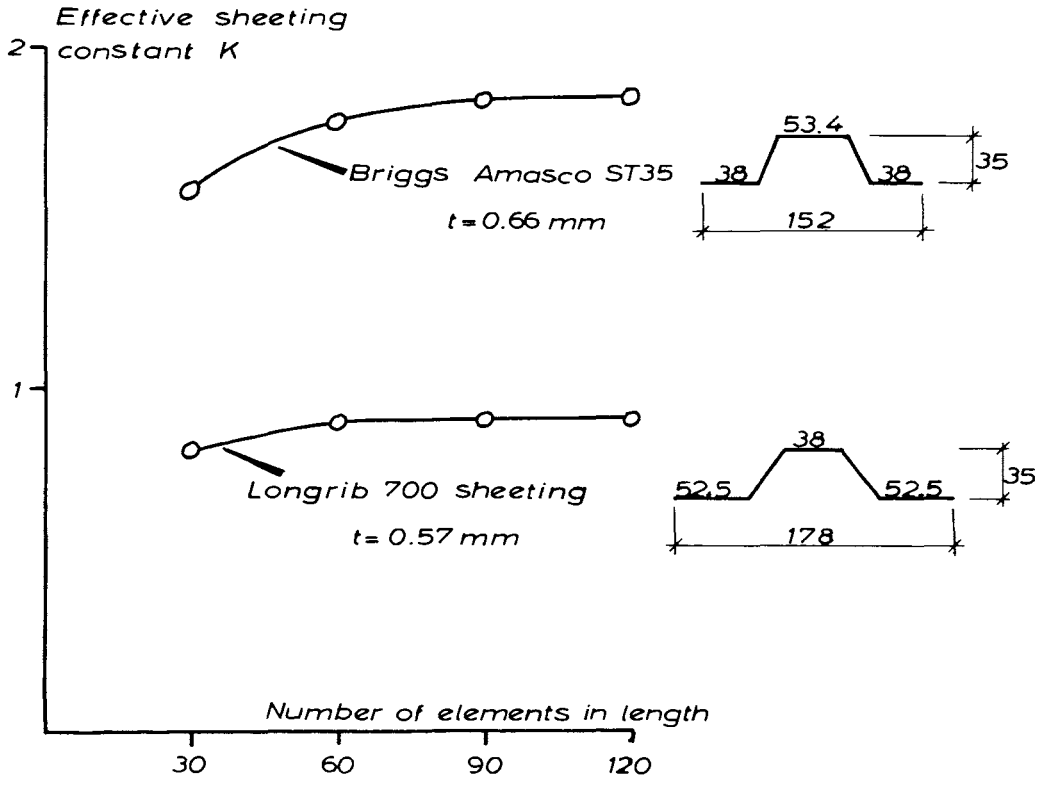

Fig 10 Convergence tests – varying number of elements in length

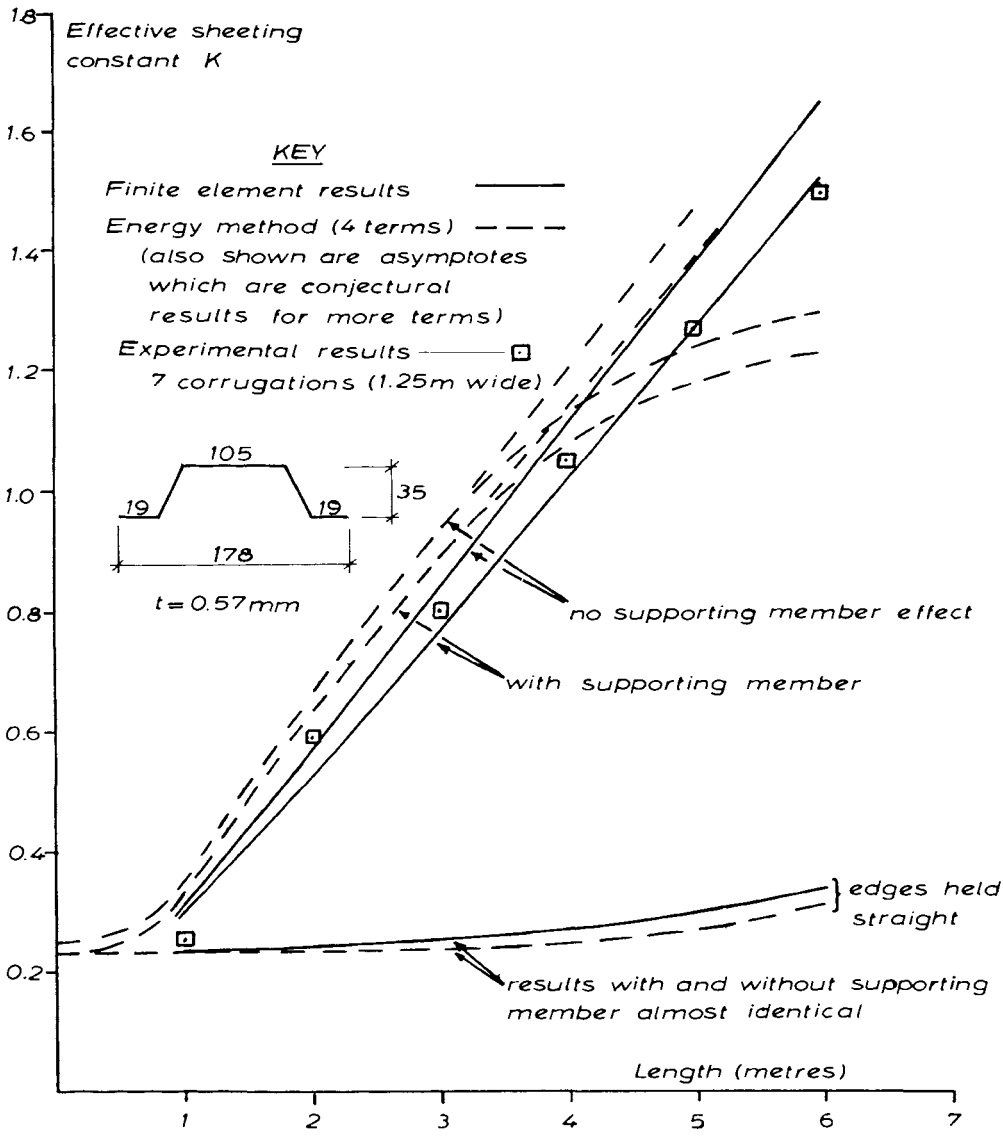

Fig 11 Summary of results Longrib 700 decking

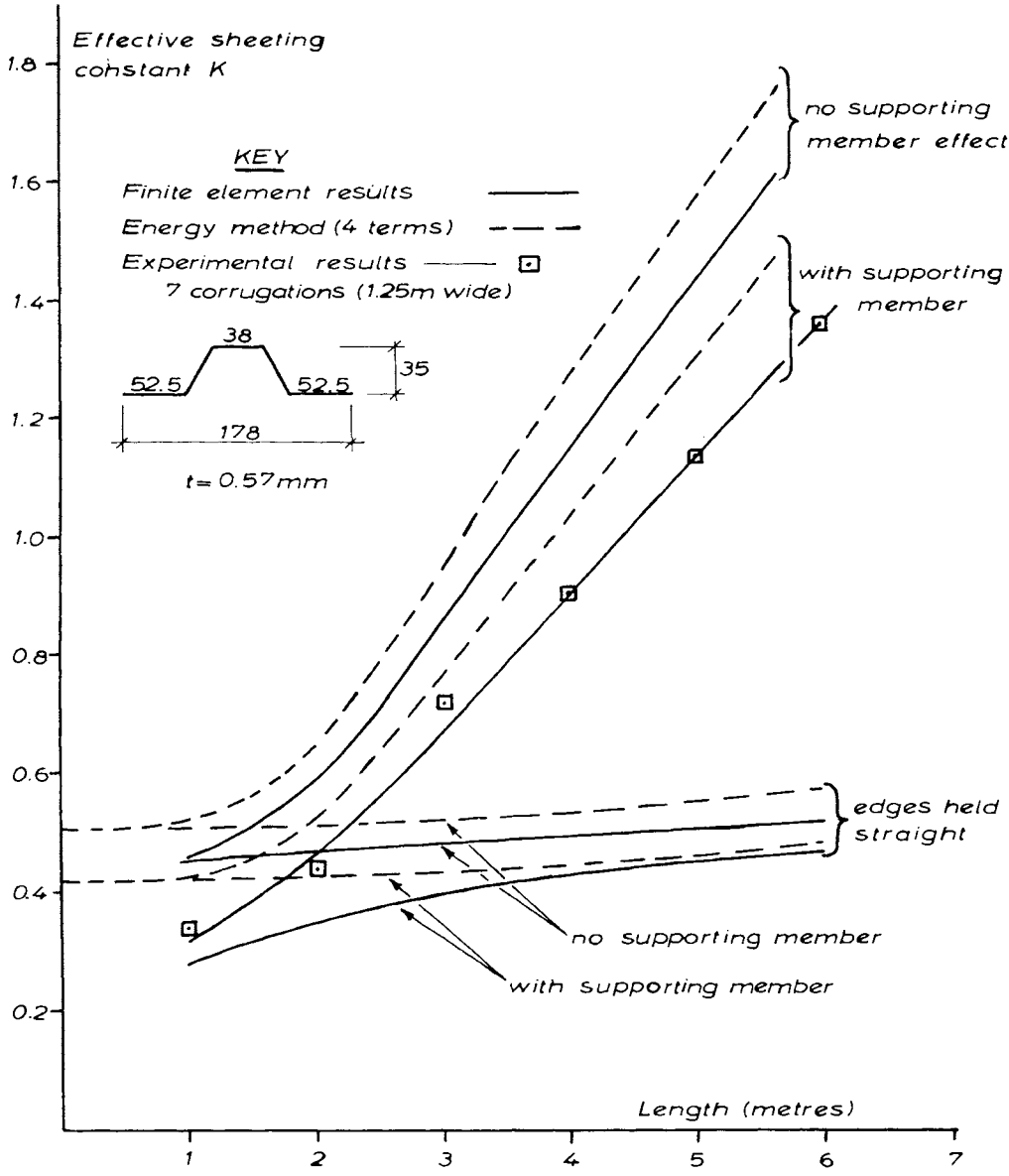

Fig 12 Summary of results Longrib 700 sheeting

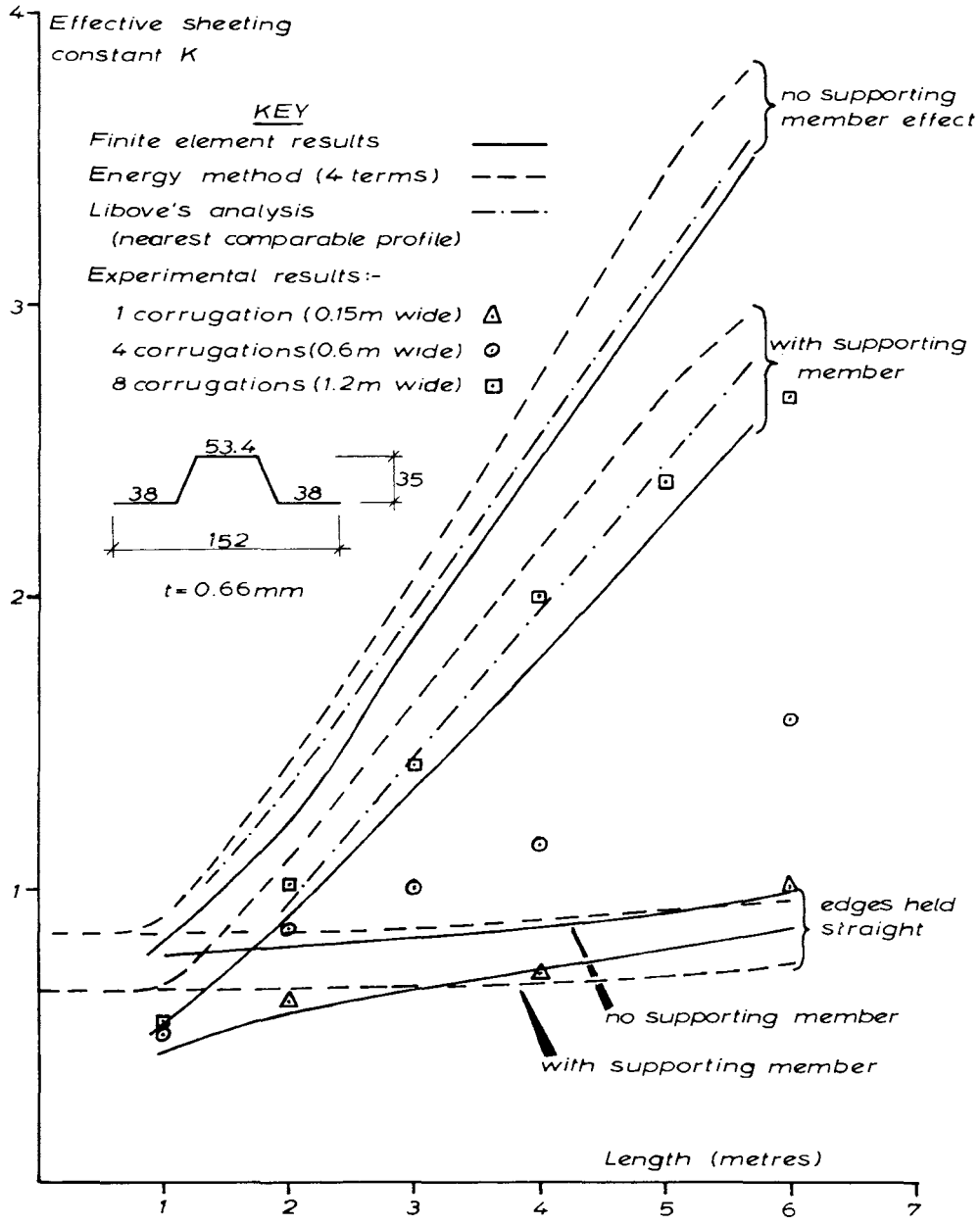

Fig 13 Summary of results — Briggs Amasco ST 35